



HHS Public Access

Author manuscript

Nature. Author manuscript; available in PMC 2014 July 10.

Published in final edited form as:

Nature. 2013 September 12; 501(7466): 179–184. doi:10.1038/nature12518.

Social reward requires coordinated activity of accumbens oxytocin and 5HT

Gül Dölen^{1,†}, Ayeh Darvishzadeh¹, Kee Wui Huang¹, and Robert C. Malenka^{1,*}

¹Nancy Pritzker Laboratory, Department of Psychiatry and Behavioral Sciences, Stanford University School of Medicine, 265 Campus Drive, Stanford CA 94305, USA

Abstract

Social behaviors in species as diverse as honey bees and humans promote group survival but often come at some cost to the individual. Although reinforcement of adaptive social interactions is ostensibly required for the evolutionary persistence of these behaviors, the neural mechanisms by which social reward is encoded by the brain are largely unknown. Here we demonstrate that in mice oxytocin (OT) acts as a social reinforcement signal within the nucleus accumbens (NAc) core, where it elicits a presynaptically expressed long-term depression of excitatory synaptic transmission in medium spiny neurons. Although the NAc receives OT receptor-containing inputs from several brain regions, genetic deletion of these receptors specifically from dorsal raphe nucleus, which provides serotonergic (5-HT) innervation to the NAc, abolishes the reinforcing properties of social interaction. Furthermore, OT-induced synaptic plasticity requires activation of NAc 5-HT_{1b} receptors, the blockade of which prevents social reward. These results demonstrate that the rewarding properties of social interaction in mice require the coordinated activity of OT and 5-HT in the NAc, a mechanistic insight with implications for understanding the pathogenesis of social dysfunction in neuropsychiatric disorders such as autism.

The mesocorticolimbic (MCL) circuit, implicated in encoding the rewarding properties of addictive drugs, likely evolved to motivate behaviors that were important for survival and reproduction. Such incentive behaviors include eating, drinking and copulation, and are reinforced by so-called ‘natural rewards’ (e.g. food, water, pheromones)¹. Growing evidence suggests that social interaction itself can act as a natural reward². However, given the diversity of social behaviors (e.g. parental investment, mating, cooperation) and the selection pressures that shaped their emergence (reproductive, predation, limited resources)³, it remains unclear whether evolutionarily conserved neural mechanisms exist to encode social reward.

Users may view, print, copy, and download text and data-mine the content in such documents, for the purposes of academic research, subject always to the full Conditions of use:http://www.nature.com/authors/editorial_policies/license.html#terms

*Correspondence to: R. Malenka, Department of Psychiatry and Behavioral Sciences, 265 Campus Drive, Room G1021, Stanford University School of Medicine, Stanford, CA 94305, Tel. 650-724-2730, Fax. 650-724-2753, malenka@stanford.edu.

†Current address: Department of Neuroscience, Johns Hopkins University, 855 N. Wolfe Street, Baltimore, MD 21205, USA

Author Contributions G.D. and R.C.M. designed the study, interpreted results and wrote the paper. G.D. performed behavioral experiments, electrophysiology, and confocal microscopy. G.D., A.D., and K.W.H. performed stereotaxic injections and immunohistochemistry. K.W.H. generated RbV viruses. All authors edited the paper.

An important clue comes from studies that have related pair-bonding behavior in prairie voles (*M. ochrogaster*) to elevated expression of oxytocin receptors (OTRs) in the nucleus accumbens (NAc), a key component of the brain's MCL reward circuit⁴. However, the species-specific nature of this mating behavior and the reported paucity of OTR expression in the NAc of mice^{2,5,6} questions the relevance of NAc OTRs to consociate social behaviors. This topic is of particular interest given that polymorphisms in the OTR gene have been associated with autism spectrum disorders, which are characterized by profound social deficits, and may be amenable to treatment with oxytocin (OT)⁷.

Mice are social animals: they live in consociate “demes” consisting of five to ten adult members that share territorial defense⁸ and alloparental responsibilities⁹ and exhibit several behaviors (e.g. vocal communication, imitation, and empathy)^{10–12} that are the hallmarks of sociality. As in several other species including humans, OT has been linked to social behaviors in mice⁷. However, OT and OTR knockout mice show a number of related behavioral deficits (i.e. memory impairment, anxiety, stress, aggressivity)⁵ making it difficult to parse the function of OT as a social reward signal in the central nervous system. To examine the hypothesis that OT signaling in mice is required for the rewarding properties of social interactions, we used a conditioned place preference (CPP) assay that has traditionally been used to study the rewarding properties of drugs of abuse¹³ and recently has been expanded to include social reward¹⁴.

Social reward requires OT

Male wild-type (WT) mice were conditioned for social CPP (Fig. 1a, b) while receiving i.p. injections of either saline or the OTR antagonist (OTR-A), L-368,899 hydrochloride (5 mg/kg, 2 days b.i.d). Saline treated WT mice showed a robust place preference for the socially conditioned context whereas OTR-A treated mice showed no preference (Fig. 1c-e). Neither locomotor activity (Supplementary Fig. 1a-i) nor cocaine CPP (Supplementary Fig. 2a-d) was altered by OTR-A treatment, demonstrating the specificity of the effects of OTR-A for the social domain. Furthermore, OTR-A, but not saline, localized to the NAc using Andalman probes (Fig. 1f, Supplementary Fig. 3a,b) prevented social CPP (Fig. 1g-i), demonstrating that OT action in the NAc is required for consociate social reward.

Given the known species and sex-specific variation in OTR expression^{2,5,15,16}, it is significant that no study to date^{6,17–19} has determined whether hypothalamic OTergic inputs to the NAc exist in male mice. Here, we injected recombinant rabies virus expressing eGFP (RbV-eGFP) into the NAc, where it is taken up by presynaptic terminals and retrogradely transported to cell bodies (Supplementary Fig. 4). In a substantial subset of hypothalamic neurons in the paraventricular nucleus (PVN), but not the supraoptic nucleus (SON), robust eGFP expression co-localizes with OT, indicating a direct axonal OTergic projection to the NAc (Supplementary Fig. 4, 5). Furthermore, these results suggest that it is the magnocellular projection from the SON that distinguishes prairie voles⁶ from rats¹⁹ and mice. Although they do not rule out an additional contribution of paracrine release, our findings demonstrate a significant synaptic source for OT in the NAc of male mice.

OT induces presynaptic LTD in NAc MSNs

To directly interrogate the synaptic role of OT within the NAc, we recorded excitatory postsynaptic currents (EPSCs) from NAc medium spiny neurons (MSNs) in acute slices. Bath application of OT (1 μ M, 10 minutes) caused a long-term depression (LTD) of EPSCs which was blocked (Fig. 2a-c) but not reversed (Fig. d-f) by the OTR antagonist (OTR-A) L-368,899 hydrochloride (1 μ M, 10 minutes). The magnitude of this OT induced LTD was significantly decreased in slices from socially conditioned versus isolation conditioned animals (Figure 2g-i), consistent with the hypothesis that social experience elicits or influences the generation of OT-LTD.

To determine if social experience preferentially influenced OT-LTD in one of the two major components of the basal ganglia circuit, direct (D1 receptor expressing) versus indirect (D2 receptor expressing) pathway MSNs²⁰, targeted recordings were made from NAc slices prepared from bacterial artificial chromosome (BAC) transgenic D1-TdTomato, and D2-eGFP reporter mice^{21,22}. Application of OT induced robust LTD (Fig. 2j-l) and isolation conditioning resulted in increased magnitude of OT-LTD (Supplementary Fig. 6) in both D1 and D2 receptor expressing MSNs, suggesting that these phenomena do not display direct and indirect pathway specificity.

To determine whether the OT-LTD was expressed pre- or postsynaptically, we performed a number of standard electrophysiological synaptic assays. The frequency, but not the amplitude of miniature EPSCs (mEPSCs), was significantly decreased by OT application (Fig. 2m-q). Furthermore, both the paired-pulse ratio of EPSCs (PPR; 50 msec inter-stimulus interval) and the coefficient of variation (CV) of the EPSCs were increased following OT application (Fig. 2r-t). Together, these findings suggest that OT-LTD results from a decrease in presynaptic neurotransmitter release probability.

Social reward requires presynaptic OTRs in NAc

Anatomical studies have revealed sparse expression of OTRs in mouse NAc^{2,5}. Moreover, immunostaining in OTR Venus Neo/+ (OTR-Venus) reporter mice²³ indicates that the small subset of cells that do express OTRs in the NAc are either inhibitory interneurons or glial cells (Supplementary Fig. 7). To test the hypothesis that OTRs in the NAc are preferentially localized to presynaptic boutons deriving from afferent inputs, we injected TdTomato-expressing RbV (RbV-TdTomato) into the NAc of OTR-Venus reporter mice (Supplementary Fig. 8). Cellular co-localization of TdTomato and Venus was detected in several, but not all, brain regions projecting to the NAc (Supplementary Fig. 8), identifying a number of putative sources of presynaptic OTRs in the NAc.

To extend the anatomical mapping of OTRs to their functional role in social reward *in vivo*, we used conditional OTR knockout (cOTR KO) mice²⁴ combined with Cre recombinase (Cre)-expressing RbV or adeno-associated virus (AAV) injected into the NAc, an approach that allowed selective ablation of pre- or postsynaptic NAc OTRs, respectively. Normal social CPP was observed in both sham injected WT and cOTR mice (Fig. 3a-d). Injection of the AAV-Cre-eGFP to delete OTRs from cells within the NAc did not affect social CPP in either WT or cOTR mice (Fig. 3e-h). Consistent with this lack of effect of deleting OTRs

from cells within the NAc, OT application did not induce long lasting changes at inhibitory synapses onto MSNs (Supplementary Fig. 9). In contrast, injection of RbV-Cre-eGFP to delete presynaptic OTRs in the NAc, completely blocked social CPP in cOTR KO mice while having no effect in WT mice (Fig. 3i-l). Injection sites and viral expression were confirmed for all animals (Supplementary Fig. 10 and 11). Considered together with the pharmacological results showing OTRs within the NAc are required for social CPP (Fig. 1f-i), these results indicate that OTRs on presynaptic boutons within the NAc are required for social reward.

sCPP and LTD require dRph inputs and 5HT1B receptors

To determine which of the afferent inputs expressing OTRs identified by RbV-mediated molecular ablation are required for social CPP, we next injected AAV-eCre-eGFP into selected brain regions of cOTR mice. Deleting OTRs in either the anterior cingulate cortex or the ventral subiculum had no effect on social CPP (Supplementary Fig. 12) while AAV-Cre-eGFP injections into the dorsal raphe nucleus (dRph) of cOTR mice, but not WT mice, prevented social CPP (Fig. 4a-d). This same manipulation also significantly reduced OT-LTD recorded ex-vivo (Fig. 4e-g). Together these results provide support for the hypothesis that presynaptic OTRs on dRph axon terminals within the NAc are specifically required for social reward.

Since the dRph is one of the major sources of serotonin (5HT) in the brain, we further characterized NAc projection neurons in the dRph and found substantial overlap between OTR- and 5HT-expressing cells (Supplementary Fig.13), raising the possibility of coordinated activity of these transmitters in the NAc. Because 5HT1b receptors have been implicated in social behaviors^{25,26} and autism²⁷ and their activation elicits a presynaptic LTD in the striatum²⁸, we hypothesized that OT may induce LTD in the NAc via activation of 5HT1b receptors. Consistent with previous results²⁸, application of the 5HT1b selective agonist CP-93129 induced robust LTD in NAc MSNs (Fig. 5a-c). Subsequent application of OT caused no further depression (Fig. 5a-c), suggesting that the 5HT1b receptor-induced LTD had occluded OT-LTD. To test whether OT-LTD required release of 5HT within the NAc, we applied the 5HT1b receptor antagonist NAS-181 (20 μ M) to NAc slices, a manipulation that largely prevented the LTD normally induced by OT (Fig. 5d-f). In contrast, 5HT1b receptor-induced LTD was readily induced in slices in which OTRs had been pharmacologically blocked (Fig. 5g-i) or molecularly ablated from dRph projections (Supplementary Fig. 14). Application of NAS-181 also prevented the decrease in mEPSC frequency normally elicited by OT (Fig. 5j-n), but had no effect on its own (Supplementary Figure 15).

Together these results support the hypothesis that activation of OTRs on the terminals of dRph axons within the NAc leads to a 5HT1b receptor-dependent form of LTD (Supplementary Fig. 16) and that this synaptic modulation is necessary for social reward, as measured by social CPP. A strong prediction of this hypothesis is that blockade of 5HT1b receptors within the NAc should prevent social CPP. Consistent with this prediction, NAS-181, but not saline, infusions into the NAc during conditioning (Fig. 6a), prevented the occurrence of social CPP (Fig. 6b-d).

Concluding remarks

We have demonstrated that the coordinated activity of OT and 5HT is required for the reward associated with social interactions and modifies MCL circuit properties by generating LTD of excitatory synapses onto MSNs in the NAc. Moreover, our findings specifically implicate OT-mediated 5HT release in the NAc in the regulation of social reward. Because OT-LTD occurs in both D1 and D2 receptor expressing MSN subtypes, as does 5HT1b-LTD²⁸, these results suggest that social reward is not expressly governed by the dichotomies proposed by prevailing models of striatal function²⁰. Indeed, the two-pathway framework for striatal function is likely oversimplified^{29–32} and computational modeling studies have proposed that reinforcement learning engages multiple neuromodulatory reward circuits in parallel³³. Furthermore, 5HT and dopamine (DA) systems may represent reward in fundamentally different ways^{34–36}. Future studies examining the interplay between DA and 5-HT in the regulation of social reward will therefore be informative.

In light of estimates that the shift to social living preceded the emergence of pair-living by 35 million years³⁷, we suggest that the NAc-dependent social reward mechanisms described here are the predecessors of evolutionary specializations seen in prairie voles^{2,5,6}. These mechanisms utilize presynaptically localized OTRs, which couple to G-proteins⁵, and thus may have been overlooked by previous studies that relied on receptor autoradiography and transcript tagging to conclude that OTRs do not exist in the NAc of consociate species like mice^{2,6}. Moreover, since it is these antecedent social behaviors that are disrupted in neuropsychiatric diseases such as autism³⁸, the elucidation of the neural mechanisms mediating social reward is a critical step toward the development of rational, mechanism-based treatments for brain disorders that involve dysfunction in social behaviors.

METHODS

Animals

Male young adult (4–6 weeks of age) C57BL/6 (Charles River), DRD1A–TdTomato BAC transgenic²¹ (D1–TdTomato, gift of N. Calakos, Duke University, Durham, NC), DRD2–eGFP BAC transgenic²² (D2–eGFP), Oxttrtm1.1Wsy homozygous²⁴ (cOTR KO, Jackson Laboratory), or OTR Venus Neo/+²³ (OTR–Venus, gift of L.J. Young, Emory University, Atlanta, GA) mice backcrossed to C57BL/6 were used for all experiments. All procedures complied with the animal care standards set forth by the National Institutes of Health and were approved by Stanford University’s Administrative Panel on Laboratory Animal Care. All animals were maintained on a 12:12 hour light:dark cycle. Experimenters were blind to the treatment condition when subjective criteria were used as a component of data analysis, and control and test conditions were interleaved for all experiments.

Behavioral Assays

The protocol for social conditioned place preference (sCPP) was shortened to 2 days of conditioning (Fig. 1a) from 10 days of conditioning^{14,39}. Animals were weaned (or delivered from Charles River) at 3 weeks of age into “home” cages containing 3–5 cage-mates, and housed on corn cob bedding (Bed-O’Cobs, 1/8”, PharmaServ). One to two weeks

later, animals were subjected to experimental manipulations and returned to their home cage (all cage-mates were of the same genotype and received the same experimental manipulation). Animals were then placed in open field activity chamber (ENV-510, Med Associates) equipped with infrared beams and a software interface (Activity Monitor, Med Associates) that monitors the position of the mouse. The apparatus was divided into two equally sized zones using a clear plastic wall, with a 5 cm diameter circular opening at the base; each zone contained one type of novel bedding (Alpha-Dri, PharmaServ, Alpha Chip, PharmaServ; Bed-O’Cobs, 1/4”, PharmaServ; or Kaytee Soft Granule, Petco). The amount of time spent freely exploring each zone was recorded during 30-minute test sessions. After an initial test (pre-conditioning trial) to establish baseline preference for the two sets of bedding cues, mice were assigned to receive social conditioning (with cage-mates) for 24 hours on one type of bedding, followed by 24 hours on the isolate bedding cue (without cage-mates) on the other type of bedding. Bedding assignments (social vs isolate) were counterbalanced for an unbiased design. 24 hours later, animals received a 30-minute post-conditioning trial to establish preference for the two conditioned cues. Animals were excluded (pre-established criteria) if they exhibited a pre-conditioning preference score >1.5 or <0.5 (for an unbiased procedure); pre-conditioning versus post-conditioning social preference scores were considered significant if paired student’s t-test P values were <0.05 . Comparisons between experimental conditions were made using both *normalized social preference scores* (time spent in social zone post over pre), and *subtracted social preference scores* (time spent in social zone post minus pre); these were considered significant if unpaired student’s t-test (two conditions), or ANOVA (three conditions, Supplementary Fig. 6) P values were <0.05 .

For cocaine-conditioned place preference (cCPP), the apparatus was divided into two equally sized zones using plastic floor tiles with distinct visual and tactile cues (grey & smooth or white & rough). After 5 days b.i.d. saline injections for habituation in the home cage, the amount of time spent freely exploring each zone was recorded during 30-minute test sessions. After an initial test to establish baseline preference for the two sets of cues, mice in each of the two treatment groups (i.p. saline or i.p. OTR-A) were randomly assigned in a counterbalanced fashion to receive cocaine (20 mg/kg) or saline in the presence of one set of cues (i.e., an unbiased design). The second conditioning session was conducted 24 hours later in the presence of the other set of cues. The post-conditioning test session was conducted 24 hours after the second conditioning session to determine time spent in the presence of the cocaine versus saline associated cue. Isolation and socially housed animals were not different in terms of cCPP so they were pooled for further analysis. Pre-conditioning, post-conditioning, subtracted, and normalized cocaine preference scores were calculated as in sCPP.

Andalman probes

Modified Andalman probes were constructed as described previously⁴⁰ (Supplementary Fig. 1e). Briefly, probes consisted of a reservoir (Polypropylene Luer Hub) attached to a double cannula guide (C235gs, 26GA, C/C distance 2.0mm, 5mm pedestal, cut 4mm below pedestal, custom specified for mouse bilateral NAc coordinates, Plastics One Inc). Polyimide tubing (40 AWG, 0.0031" ID, 0.0046" OD, 0.00075" Wall, Small Parts) was

threaded through the stainless steel tubing of the cannula guide on one end, and out of a hole drilled into the luer hub to act as a flush outlet (outflow tube) on the other end. The dialysis membrane (Spectra/Por, 13 kD molecular weight cut-off, Spectrum Labs) was then threaded over the outflow tube and through the cannula guide; ends were cut such that ~ 500 μ m of dialysis membrane was exposed below the cannula guide and above the sealed end. Junctions were sealed with bio-compatible epoxies (Epo-Tek 730, Epo-Tek 301, Epoxy Technologies). In this design, a pharmacological agent could be intracranially delivered rapidly, continually, and concurrently to all members of the social group, without anesthesia.

At postnatal day 35 - 40, probes were implanted into the NAc of male mice following bilateral craniotomy (bregma 1.54 mm; lateral 1.0 mm) and attached to the skull using dental acrylic. Previous reports indicate that for complete pharmacological effect, drug concentration in the reservoir must be ~500 times the dose used for direct injections^{40,41}, thus OTR and 5HT_{1b} antagonists were applied at 10 mM (L-368,899) and 85 mM (NAS-181) in a volume of 25 μ l saline. Probe placement and competency was verified by post-hoc application of concentrated Fluorescein sodium salt (Sigma-Aldrich) to reservoir prior to intracardial PFA perfusion and histology (Supplementary Fig. 1f).

Virus Generation

Rabies virus (RbV) was generated from a full length cDNA plasmid containing all components of RbV (SAD L16; gift from Dr. Karl-Klaus Conzelmann, University of Munich, Germany)⁴². We replaced the rabies virus glycoprotein with eGFP (RbV-eGFP), TdTomato (RbV-TdTomato) or Cre-eGFP to generate RbV expressing Cre-eGFP (RbV-Cre-eGFP), eGFP (RbV-eGFP) or TdTomato (RbV-TdTomato). To rescue RbV from this cDNA we used a modified version of a published protocol^{42,43}. Briefly, HEK293T cells were transfected with a total of 6 plasmids; 4 plasmids expressing the RbV components pTIT-N, pTIT-P, pTIT-G, and pTIT-L; one plasmid expressing T7 RNA polymerase (pCAGGS-T7), and the aforementioned glycoprotein-deleted RbV cDNA plasmid expressing Cre-eGFP, eGFP or TdTomato. For the amplification of RbV, the media bathing these HEK293T (ATCC) cells was collected 3-4 days posttransfection and moved to baby hamster kidney (BHK) cells stably expressing RbV glycoprotein (BHK-B19G)⁴⁴. After three days, the media from BHK-B19G cells was collected, centrifuged for 5 min at 3,000 X g to remove cell debris, and concentrated by ultracentrifugation (55,000 X g for 2 hr). Pellets were suspended in DPBS, aliquoted and stored at -80°C. The titer of concentrated RbV was measured by infecting HEK293 cell and monitoring fluorescence. Plasmids expressing the RbV components were gifts from Dr. Karl-Klaus Conzelmann and Dr. Ian Wickersham (Massachusetts Institute of Technology, MA). BHK cells stably expressing B19G were a gift from Dr. Edward Callaway (Salk Institute, La Jolla, CA).

The adeno-associated viruses (AAVs) used in this study were produced by the Stanford Neuroscience Gene Vector and Virus Core. Briefly, AAV-DJ⁴⁵ was produced by transfection of AAV 293 cells (Agilent, Inc) with three plasmids: an AAV vector expressing Cre-eGFP, AAV helper plasmid (pHELPER, Agilent, Inc), and AAV rep-cap helper plasmid (pRC-DJ, gift from Mark Kay, Stanford). At 72 h after transfection, the cells were harvested and lysed by a freeze-and-thaw procedure. Viral particles were then purified by an iodixanol

step gradient ultracentrifugation method. The iodixanol was diluted and the AAV was concentrated using a 100 kDa molecular weight cutoff ultrafiltration device. The genomic titer was determined by Q-PCR.

Stereotaxic injections

Stereotaxic injection of viruses into NAc was performed under general ketamine-medetomidine anesthesia using a stereotaxic instrument (David Kopf). A small volume (~1 μ l) of concentrated virus solution was injected bilaterally into NAc core (bregma 1.54 mm; lateral 1.0 mm; ventral 4.0 mm), unilaterally into the dorsal Raphe (dRph; bregma -3.3 mm; lateral 0.0 mm; ventral 3.35 mm), bilaterally into the ventral subiculum (vSub; bregma -2.95 mm; lateral 3.1 mm; ventral 4.35 mm), or bilaterally anterior cingulate (ACC; bregma 1.0 mm; lateral 0.3 mm; ventral 1.25 mm) at a slow rate (100 nl/min) using a syringe pump (Harvard Apparatus, MA). The injection needle was withdrawn 5 min after the end of the infusion. Animals were tested 7 days after AAV or RbV injections. Injection sites and viral infectivity were confirmed in all animals post-hoc by preparing sections (50 μ m) containing the relevant brain region (Supplementary Fig. 9).

Immunohistochemistry

Immunohistochemistry and confocal microscopy were performed as described previously⁴⁶. Briefly, after intracardial perfusion with 4% paraformaldehyde in PBS (pH 7.4), the brains were post fixed overnight in this same solution and the following day 50 μ M coronal, sagittal, or horizontal sections were prepared. Primary antibodies were used at the following concentrations: mouse anti-oxytocin-neurophysin (OT-np, 1:50; Gift of Harold Gainer, NIH Bethesda, MD^{47,48}); rat anti-green fluorescent protein (GFP, 1:1000; Nacalai); rabbit anti-parvalbumin (PARV, 1:750; Swant); rabbit anti-neuronal nitric oxide synthase (nNOS, 1:100; BD Transduction Laboratories); rabbit anti-glial fibrillary protein (GFAP, 1:80; Sigma-Aldrich); rabbit anti-choline acetyltransferase (CHAT, 1:100; Millipore); rabbit anti-dopamine receptor protein (DARP, 1:100, Millipore); sheep anti-tryptophan hydroxylase (TrypH, 1:100 Millipore) diluted in a solution containing 1% horse serum, 0.2% BSA, and 0.5% Triton X-100 in PBS. After overnight incubation in primary antibody (RT, shaker), slices were washed four times in PBS and then incubated with appropriate secondary antibody diluted at 1:750 for 2 h in PBS containing 0.5% Triton X-100. Subsequently, slices were washed 5 times and mounted using Vectashield mounting medium (Vector Laboratories). To identify cells expressing GFP or TdTomato due to the injection of RbV-eGFP or RbV-TdTomato into the NAc, raw fluorescence was visualized. Image acquisition was performed with a confocal microscope (Zeiss LSM510) using a 10x/0.30 Plan Neofluar and a 40x/1.3 Oil DIC Plan Apochromat objective. Confocal images were examined using the Zeiss LSM Image Browser software.

Electrophysiology

Parasagittal slices (250 μ m) containing the NAc core were prepared from C57BL/6 and D1-TdTomato/D2-eGFP BAC transgenic mice on a C57BL/6 background using standard procedures. Briefly, after mice were anesthetized with isoflurane and decapitated, brains were quickly removed and placed in ice-cold low sodium, high sucrose dissecting solution. Slices were cut by adhering the two sagittal hemispheres brain containing the NAc core to

the stage of a Leica vibroslicer. Slices were allowed to recover for a minimum of 60 min in a submerged holding chamber (~25°C) containing artificial cerebrospinal fluid (ACSF) consisting of 119 mM NaCl, 2.5 mM KCl, 2.5 mM CaCl₂, 1.3 mM MgSO₄, 1 mM NaH₂PO₄, 11 mM glucose and 26.2 mM NaHCO₃. Slices were then removed from the holding chamber and placed in the recording chamber where they were continuously perfused with oxygenated (95% O₂, 5% CO₂) ACSF at a rate of 2 ml per min at 26 ± 2°C. For EPSC recordings, bicuculline (20 μM) was added to the ACSF to block GABA_A receptor-mediated inhibitory synaptic currents. For IPSC recordings, dl-2-amino-5-phosphonovalerate (dAPV, 10 μM) and 2,3-Dioxo-6-nitro-1,2,3,4-tetrahydrobenzo[f]quinoxaline-7-sulfonamide (NBQX, 5 μM) dissolved in DMSO were added to block NMDA and AMPA receptors respectively. Whole-cell voltage-clamp recordings from MSNs were obtained under visual control using a 40X objective. The NAc core was identified by the presence of the anterior commissure. D1- and D2 MSNs in the NAc core were identified by the presence of TdTomato and eGFP, respectively, that were excited with UV light using bandpass filters (HQ545/30x EX for TdTomato; HQ470/40x EX for eGFP). Recordings were made with electrodes (3.5–6.5 MΩ) filled with 115 mM CsMeSO₄, 20 mM CsCl, 10 mM HEPES, 0.6 mM EGTA, 2.5 mM MgCl, 10 mM Na-phosphocreatine, 4 mM Na-ATP, 0.3 mM Na-GTP, and 1 mM QX-314. Excitatory and inhibitory afferents were stimulated with a bipolar nichrome wire electrode placed at the border between the NAc core and cortex dorsal to the anterior commissure. Recordings were performed using a Multiclamp 700B (Molecular Devices), filtered at 2 kHz and digitized at 10 kHz. EPSCs were evoked at a frequency of 0.1 Hz while MSNs were voltage-clamped at -70 mV. Data acquisition and analysis were performed on-line using custom Igor Pro software. Input resistance and access resistance were monitored continuously throughout each experiment; experiments were terminated if these changed by >15%.

Summary LTD graphs were generated by averaging the peak amplitudes of individual EPSCs in 1 min bins (6 consecutive sweeps) and normalizing these to the mean value of EPSCs collected during the 10 min baseline immediately before the LTD-induction protocol. Individual experiments were then averaged together. Oxytocin (OT, Tocris Biosciences, 1 μM, 10 minute) was bath applied following the collection of baseline for induction of OT-LTD. For experiments examining the blockade of OT-LTD, slices were pre-incubated in antagonist (OTR-A, 1 μM L-368,899 hydrochloride or 5HT1b-A, 20 μM NAS-181; Tocris Biosciences) for at least 30 minutes prior to recording. For experiments examining the reversal of OT-LTD, 30-40 minutes post induction, OTR-A was bath applied for 10 minutes. Following the collection of stable baseline EPSCs, 5HT1b-LTD was induced by 10 minute bath application of 2 μM CP-93129 dihydrochloride (Tocris Biosciences) as described previously²⁸. For experiments examining the occlusion of OT-LTD, after stabilization of 5HT1b-LTD (at 30-40 minutes post induction), 1 μM OT was bath applied for 10 minutes. Miniature EPSCs were collected at a holding potential of -70 mV in the presence of TTX (0.5 μM). 2 minutes after break-in (sweep number 5, 30s sweeps), thirty second blocks of events (total of 200 events per cell) were acquired and analyzed using Mini-analysis software (Synaptosoft) with threshold parameters set at 5 pA amplitude and <3 ms rise time. All events included in the final data analysis were verified by eye. Slices were incubated in the appropriate drug (dissolved in ACSF-bicuculline) for 10 minutes prior

to recording, and cross-cell comparisons were made. Paired-pulse ratios (PPR) were acquired by applying a second afferent stimulus of equal intensity, 50 ms after the first stimulus, and then calculating the ratio of EPSC2/EPSC1. Coefficient of variance (CV) was calculated from the standard deviation divided by the average (STDEV/AVG) of 10-minute blocks (minutes 0-10, pre; minutes 40-50, post). Comparisons between different experimental manipulations were made using a two-tailed, Students T-test (paired or unpaired, as appropriate) with $P < 0.05$ considered significant. All statements in the text regarding differences between grouped data indicate that statistical significance was achieved, assuming normal distribution and equal variance. Sample size was estimated based on published literature^{14,28}. All values are reported as mean \pm s.e.m.

Supplementary Material

Refer to Web version on PubMed Central for supplementary material.

Acknowledgments

We thank members of the Malenka laboratory for comments, A. Andalman, W. Xu, B.K. Lim and T. Sudhof for technical advice, as well as the SIM1 Animal Care facility for husbandry support. The OT-neurophysin antibody was a gift of H. Gainer. OTR-Venus reporter mice were a gift of L.J. Young. D1-TdTomato BAC transgenic mice were provided by N. Calakos. The rabies virus complementary DNA plasmid and viral component-expressing plasmids were gifts from K. Conzelmann and I. Wickersham. HHK-B19G cells were a gift from E. Callaway. AAVs were produced by the Stanford NGVVC (supported by National Institutes of Health grant NIH NS069375). The AAV-DJ helper plasmid was a gift from M. Kay. Supported by funding from the Simons Foundation Autism Research Initiative (R.C.M.), N.I.H. (R.C.M.), and a Berry Foundation Postdoctoral Fellowship (G.D)

References

1. Kelley AE, Berridge KC. The neuroscience of natural rewards: relevance to addictive drugs. *J Neurosci.* 2002; 22:3306–3311. [PubMed: 11978804]
2. Insel TR. Is social attachment an addictive disorder? *Physiol Behav.* 2003; 79:351–357. [PubMed: 12954430]
3. Shultz S, Opie C, Atkinson QD. Stepwise evolution of stable sociality in primates. *Nature.* 2011; 479:219–222. [PubMed: 22071768]
4. Young LJ, Wang Z. The neurobiology of pair bonding. *Nature Neurosci.* 2004; 7:1048–1054. [PubMed: 15452576]
5. Lee HJ, Macbeth AH, Pagani JH, Young WS. Oxytocin: the great facilitator of life. *Prog Neurobiol.* 2009; 88:127–151. [PubMed: 19482229]
6. Ross HE, et al. Characterization of the oxytocin system regulating affiliative behavior in female prairie voles. *Neurosci.* 2009; 162:892–903.
7. Yamasue H, et al. Integrative approaches utilizing oxytocin to enhance prosocial behavior: from animal and human social behavior to autistic social dysfunction. *J Neurosci.* 2012; 32:14109–14117. [PubMed: 23055480]
8. Anderson PK, Hill J. *Mus musculus*: experimental induction of territory formation. *Science.* 1965; 148:1753–1755. [PubMed: 17819441]
9. Riedman ML. The evolution of alloparental care and adoption in mammals and birds. *Quart Rev Biol.* 1982; 57:405–435.
10. Holy TE, Guo Z. Ultrasonic songs of male mice. *PLoS Biol.* 2005; 3:e386. [PubMed: 16248680]
11. Panksepp J. Behavior. Empathy and the laws of affect. *Science.* 2011; 334:1358–1359. [PubMed: 22158811]

12. Hodgson SR, Hofford RS, Roberts KW, Wellman PJ, Eitan S. Socially induced morphine pseudosensitization in adolescent mice. *Behav Pharmacol.* 2010; 21:112–120. [PubMed: 20215964]
13. Tzschentke TM. Measuring reward with the conditioned place preference (CPP) paradigm: update of the last decade. *Addiction Biol.* 2007; 12:227–462.
14. Panksepp JB, Lahvis GP. Social reward among juvenile mice. *Genes, Brain, Behav.* 2007; 6:661–671. [PubMed: 17212648]
15. Rosen GJ, de Vries GJ, Goldman SL, Goldman BD, Forger NG. Distribution of oxytocin in the brain of a eusocial rodent. *Neurosci.* 2008; 155:809–817.
16. Hermes ML, Buijs RM, Masson-Pévet M, Pévet P. Oxytocinergic innervation of the brain of the garden dormouse (*Eliomys quercinus* L.). *J Comp Neurol.* 1988; 273:252–262. [PubMed: 3417903]
17. Phillipson OT, Griffiths AC. The topographic order of inputs to nucleus accumbens in the rat. *Neurosci.* 1985; 16:275–296.
18. Brog JS, Ongse AS, Deutch AY, Zahm DS. The patterns of afferent innervation of the core and shell in the “accumbens” part of the rat ventral striatum: immunohistochemical detection of retrogradely transported fluoro-gold. *J Comp Neurol.* 1993; 278:255–278. [PubMed: 8308171]
19. Knobloch HS, et al. Evoked axonal oxytocin release in the central amygdala attenuates fear response. *Neuron.* 2012; 73:553–566. [PubMed: 22325206]
20. Lobo MK, Nestler EJ. The striatal balancing act in drug addiction: distinct roles of direct and indirect pathway medium spiny neurons. *Front Neuroanat.* 2011; 5:41. [PubMed: 21811439]
21. Shuen, Ja; Chen, M.; Gloss, B.; Calakos, N. *Drd1a-tdTomato* BAC transgenic mice for simultaneous visualization of medium spiny neurons in the direct and indirect pathways of the basal ganglia. *J Neurosci.* 2008; 28:2681–2685. [PubMed: 18337395]
22. Gong S, et al. A gene expression atlas of the central nervous system based on bacterial artificial chromosomes. *Nature.* 2003; 425:917–925. [PubMed: 14586460]
23. Yoshida M, et al. Evidence that oxytocin exerts anxiolytic effects via oxytocin receptor expressed in serotonergic neurons in mice. *J Neurosci.* 2009; 29:2259–2271. [PubMed: 19228979]
24. Lee HJ, Caldwell HK, Macbeth AH, Tolu SG, Young WS. A conditional knockout mouse line of the oxytocin receptor. *Endocrinology.* 2008; 149:3256–3263. [PubMed: 18356275]
25. Brunner D, Buhot MC, Hen R, Hofer M. Anxiety, motor activation, and maternal-infant interactions in 5HT1B knockout mice. *Behav Neurosci.* 1999; 113:587–601. [PubMed: 10443785]
26. Furay AR, McDevitt Ra, Miczek Ka, Neumaier JF. 5-HT1B mRNA expression after chronic social stress. *Behav Brain Res.* 2011; 224:350–357. [PubMed: 21718722]
27. Orabona GM, et al. HTR1B and HTR2C in autism spectrum disorders in Brazilian families. *Brain Res.* 2009; 1250:14–19. [PubMed: 19038234]
28. Mathur BN, Capik NA, Alvarez Va, Lovinger DM. Serotonin induces long-term depression at corticostriatal synapses. *J Neurosci.* 2011; 31:7402–11. [PubMed: 21593324]
29. Cui G, et al. Concurrent activation of striatal direct and indirect pathways during action initiation. *Nature.* 2013; 494:238–42. [PubMed: 23354054]
30. Capper-Loup C, Canales JJ, Kadaba N, Graybiel AM. Concurrent activation of dopamine D1 and D2 receptors is required to evoke neural and behavioral phenotypes of cocaine sensitization. *J Neurosci.* 2002; 22:6218–6227. [PubMed: 12122080]
31. Nambu A. Seven problems on the basal ganglia. *Curr Opin Neurobiol.* 2008; 18:595–604. [PubMed: 19081243]
32. Perreault ML, Hasbi A, O’Dowd BF, George SR. The dopamine d1-d2 receptor heteromer in striatal medium spiny neurons: evidence for a third distinct neuronal pathway in Basal Ganglia. *Front Neuroanat.* 2011; 5:31. [PubMed: 21747759]
33. Doya K. Metalearning and neuromodulation. *Neural Networks.* 2002; 15:495–506. [PubMed: 12371507]
34. Nakamura K, Matsumoto M, Hikosaka O. Reward-dependent modulation of neuronal activity in the primate dorsal raphe nucleus. *J Neurosci.* 2008; 28:5331–5343. [PubMed: 18480289]
35. Tanaka SC, et al. Prediction of immediate and future rewards differentially recruits cortico-basal ganglia loops. *Nature Neurosci.* 2004; 7:887–893. [PubMed: 15235607]

36. Boureau YL, Dayan P. Opponency revisited: competition and cooperation between dopamine and serotonin. *Neuropsychopharmacol.* 2011; 36:74–97.
37. Shultz S, Opie C, Atkinson QD. Stepwise evolution of stable sociality in primates. *Nature.* 2011; 479:219–222. [PubMed: 22071768]
38. Silverman JL, Yang M, Lord C, Crawley JN. Behavioural phenotyping assays for mouse models of autism. *Nature Rev Neurosci.* 2010; 11:490–502. [PubMed: 20559336]
39. Panksepp JB, et al. Affiliative behavior, ultrasonic communication and social reward are influenced by genetic variation in adolescent mice. *PLoS One.* 2007; 2:e351. [PubMed: 17406675]
40. Aronov D, Andalman AS, Fee MS. A specialized forebrain circuit for vocal babbling in the juvenile songbird. *Science.* 2008; 320:630–634. [PubMed: 18451295]
41. Andalman AS, Fee MS. A basal ganglia-forebrain circuit in the songbird biases motor output to avoid vocal errors. *Proc Nat Acad Sci USA.* 2009; 106:12518–12523. [PubMed: 19597157]
42. Mebatsion T, König M, Conzelmann KK. Budding of rabies virus particles in the absence of the spike glycoprotein. *Cell.* 1996; 84:941–951. [PubMed: 8601317]
43. Wickersham IR, Sullivan Ha, Seung HS. Production of glycoprotein-deleted rabies viruses for monosynaptic tracing and high-level gene expression in neurons. *Nature Prot.* 2010; 5:595–606.
44. Wickersham IR, Finke S, Conzelmann K, Callaway EM. Retrograde neuronal tracing with a deletion- mutant rabies virus. *Nature Meth.* 2007; 4:47–49.
45. Grimm D, et al. In vitro and in vivo gene therapy vector evolution via multispecies interbreeding and retargeting of adeno-associated viruses. *J Virol.* 2008; 82:5887–5911. [PubMed: 18400866]
46. Lammel S, et al. Input-specific control of reward and aversion in the ventral tegmental area. *Nature.* 2012; 491:212–217. [PubMed: 23064228]
47. Ben-Barak Y, Russell J, Whitnall M, Ozato K, Gainer H. Neurophysin in the hypothalamo-neurohypophysial system. I production and characterization of monoclonal antibodies. *J Neurosci.* 1985; 5:81–97. [PubMed: 3880813]
48. Whitnall M, Key S, Ben-Barak Y, Ozato K, Gainer H. Neurophysin in the hypothalamo-neurohypophysial system. II. immunocytochemical studies of the ontogeny of oxytocinergic and vasopressinergic neurons. *J Neurosci.* 1985; 5:98–109. [PubMed: 3880814]

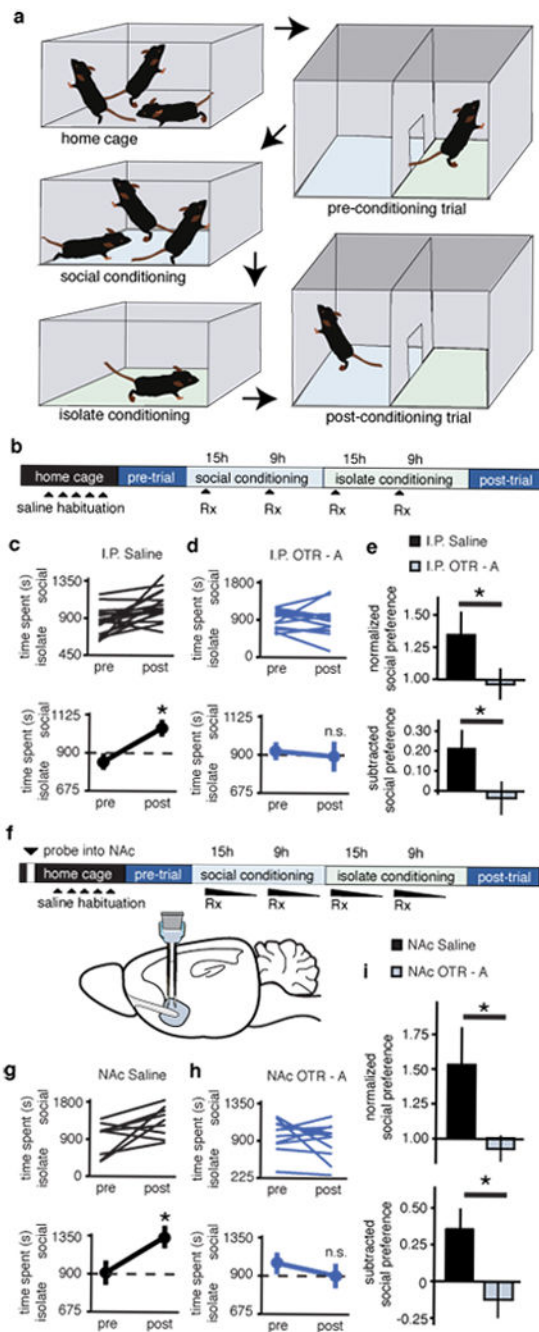


Figure 1. Oxytocin is required for sCPP

a, Protocol for sCPP. **b,f**, Experimental time course of i.p injections (**b**) and NAc reverse microdialysis (**f**) in sCPP. **c,d,g,h** Individual (top) and average (bottom) responses in animals receiving i.p. (**c**) or NAc (**g**) saline versus animals receiving i.p. (**d**) or NAc (**h**) OTR-A. For both i.p. and NAc delivery routes, saline, but not OTR-A treated, animals spend more time in social bedding cue following conditioning (n = 18 i.p. saline, n = 15 i.p. OTR-A; n = 9 NAc saline and n = 11 NAc OTR-A animals). **e,i**, Comparisons between treatment groups reveal significantly decreased normalized and subtracted social preference in both

i.p. and NAc OTR-A treated animals. Summary data are presented as mean \pm s.e.m (*p<0.05, Student's t-test).

Author Manuscript

Author Manuscript

Author Manuscript

Author Manuscript

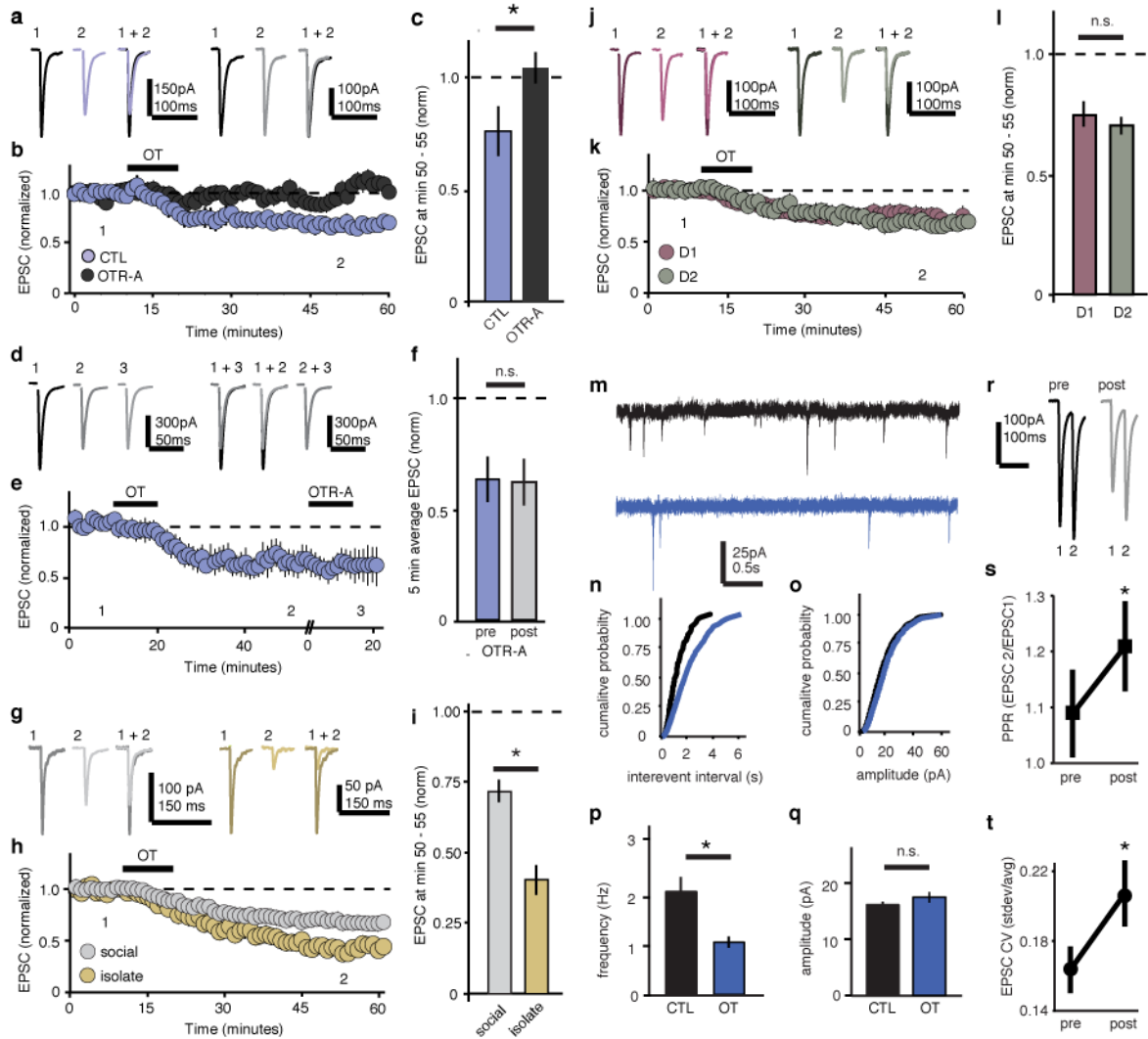


Figure 2. OT induces LTD in the NAc

a-h, Representative traces (**a,d,g,j**), summary time course (**b,e,h,k**), and average post-treatment magnitude comparisons (**c,f,i,l**) reveal significant EPSC response depression in OT treated but not OTR-A preincubated cells (**a-c**, $n = 6$ OT, $n = 6$ OT+ OTR-A preincubation cells); OT-response depression is not reversed by post-induction OTR-A chase (**d-f**, $n = 7$ cells); the magnitude of OT-LTD is significantly increased in cells from isolation versus socially reared animals (**g-i**, isolate, $n = 14$, social $n = 27$ cells); and the magnitude of EPSC OT-LTD is not different in D1 versus D2 MSNs (**j-l**, $n = 9$ D1, and $n = 11$ D2 cells). **m-q** Representative mEPSC traces (**m**), cumulative probability (**n,o**), and average (**p,q**) comparisons reveal mEPSC frequency (**n,p**), but not amplitude (**o,q**), is decreased in OT-treated versus control cells (control, $n = 11$, OT, $n = 11$ cells). **r-t**, Comparisons of representative traces (**r**) and average (**s**) paired pulse ratios PPR ($n = 6$ cells) as well as average (**t**) coefficient of variance, CV ($n = 32$ cells) reveal significant increases following induction of OT-LTD. Summary data are presented as mean \pm s.e.m (* $p < 0.05$, Student's t-test).

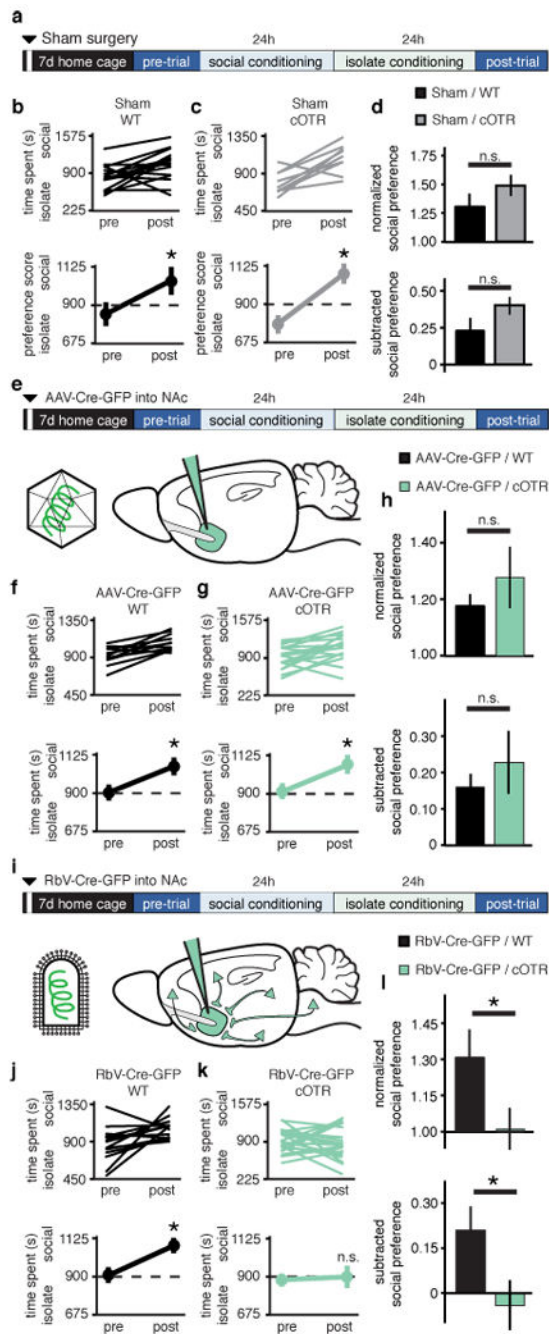


Figure 3. Presynaptic OTRs are required for sCPP

a,e,i Experimental time course for **(a)** sham, **(e)** NAc-AAV-Cre-eGFP, and **(i)** NAc-RbV-Cre-eGFP injections. **b,c,f,g,j,k**, Individual (top) and average (bottom) responses in WT **(b,f,j)**, versus cOTR **(c,g,k)** animals receiving sham **(b,c)**, NAc-AAV-Cre-eGFP **(f,g)**, or NAc-RbV-Cre-eGFP **(j,k)**. WT animals, as well as sham and NAc-AAV-Cre-eGFP injected cOTR animals, but not cOTR animals injected with NAc-RbV-Cre-eGFP, spend more time in social bedding cue following conditioning (sham WT, $n = 15$, cOTR, $n = 8$; NAc-AAV-Cre-eGFP WT, $n = 15$, cOTR, $n = 19$; NAc-RbV-Cre-eGFP WT, $n = 14$, cOTR, $n = 22$).

d,h,i, Comparisons between WT and cOTR animals reveal normal sCPP in sham and NAc-AAV-Cre-eGFP injected animals, while in NAc-RbV-Cre-eGFP injected animals sCPP is significantly decreased in cOTR versus WT controls. Summary data are presented as mean \pm s.e.m (* $p < 0.05$, Student's t-test).

Author Manuscript

Author Manuscript

Author Manuscript

Author Manuscript

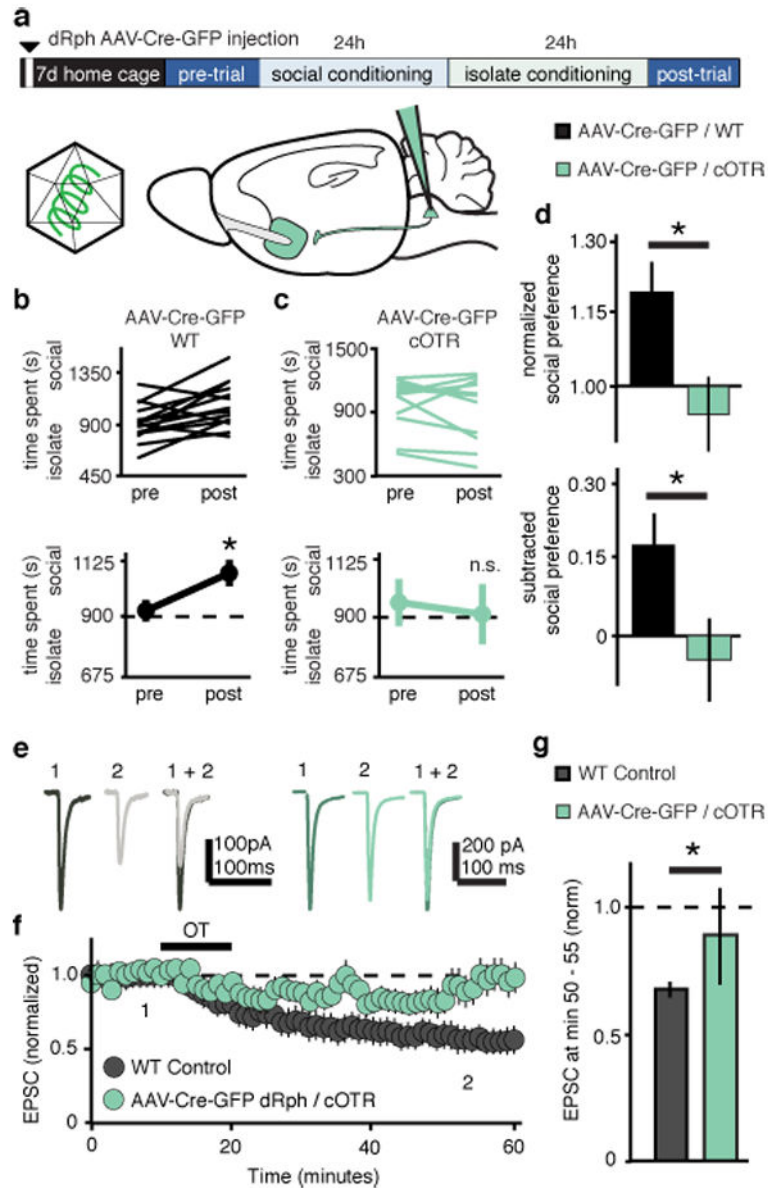


Figure 4. OTRs in dRph inputs to NAc are required for sCPP and OT-LTD

a, Experimental time course of dRph-AAV-Cre-eGFP injections in sCPP. **b,c** Individual (top) and average (bottom) comparisons reveal that dRph-AAV-Cre-eGFP injected WT (**b**), but not cOTR (**c**) animals spend significantly more time in the social bedding cue following conditioning (WT, $n = 14$, cOTR, $n = 10$). **d**, Comparisons between dRph-AAV-Cre-eGFP injected groups reveal significantly decreased sCPP in cOTR animals compared to WT controls. **e-g**, Representative traces (**e**), summary time course (**f**) and average post-treatment magnitude comparisons (**g**) reveal absence of OT-LTD in EPSCs recorded from AAV-Cre-eGFP dRph injected cOTR KO versus pooled WT control animals (dRph-AAV-Cre-eGFP injected cOTR, $n = 6$ cells; pooled WT control, $n = 30$ cells). Summary data are presented as mean \pm s.e.m (* $p < 0.05$, Student's t-test).

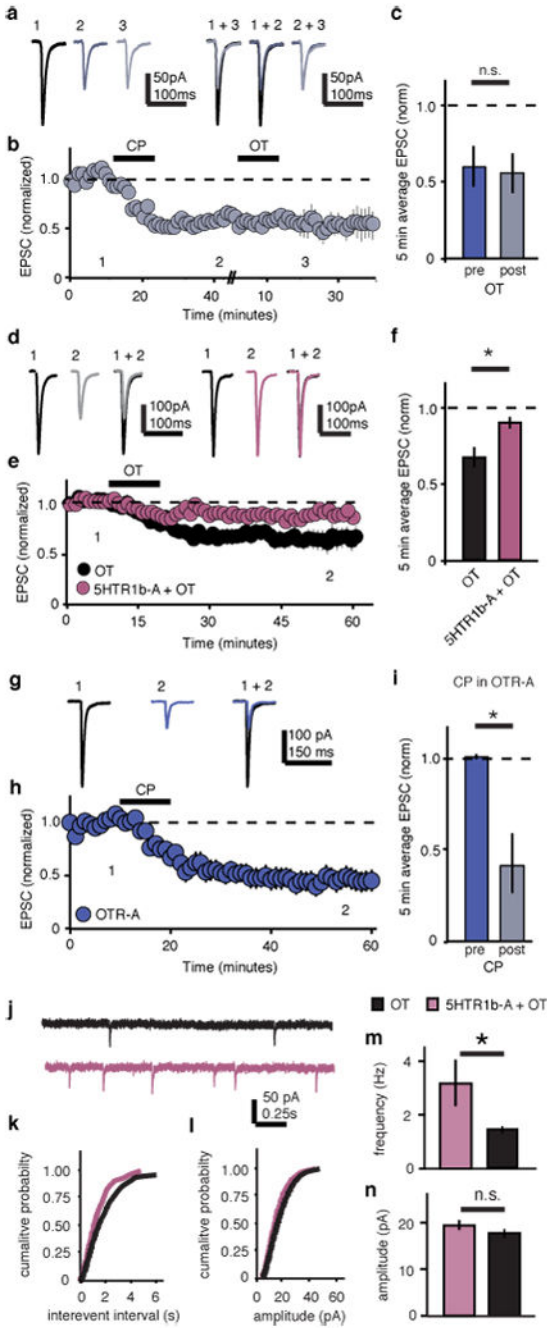


Figure 5. OT-LTD in NAc requires 5HT1b receptors

a-i, Representative traces (**a,d,g**), summary time course (**b,e,h**), and average post-treatment magnitude comparisons (**c,f,i**) reveal EPSC depression in 5HT1b agonist (CP-93129 dihydrochloride) treated cells is not augmented by subsequent application of OT (**a-c**, $n = 5$ cells); OT-LTD is significantly reduced in cells pre-treated with the 5HT1b-antagonist (NAS-181) (**d-f**, control, $n = 7$, 5HT1b antagonist, $n = 7$ cells); CP-LTD is induced in slices in which OTRs are pharmacologically blocked (**g-i**, $n = 5$ cells). **j-n** Representative mEPSC traces (**j**), cumulative probability (**k,l**), and average (**m,n**) comparisons reveal

mEPSC frequency (**k,m**), but not amplitude (**l,n**), is decreased in OT-treated cells versus cells treated with OT in the presence of NAS-181 (OT, n = 17 cells, OT + 5HTR1b-A, n = 17 cells). Summary data are presented as mean \pm s.e.m (*p<0.05, Student's t-test).

Author Manuscript

Author Manuscript

Author Manuscript

Author Manuscript

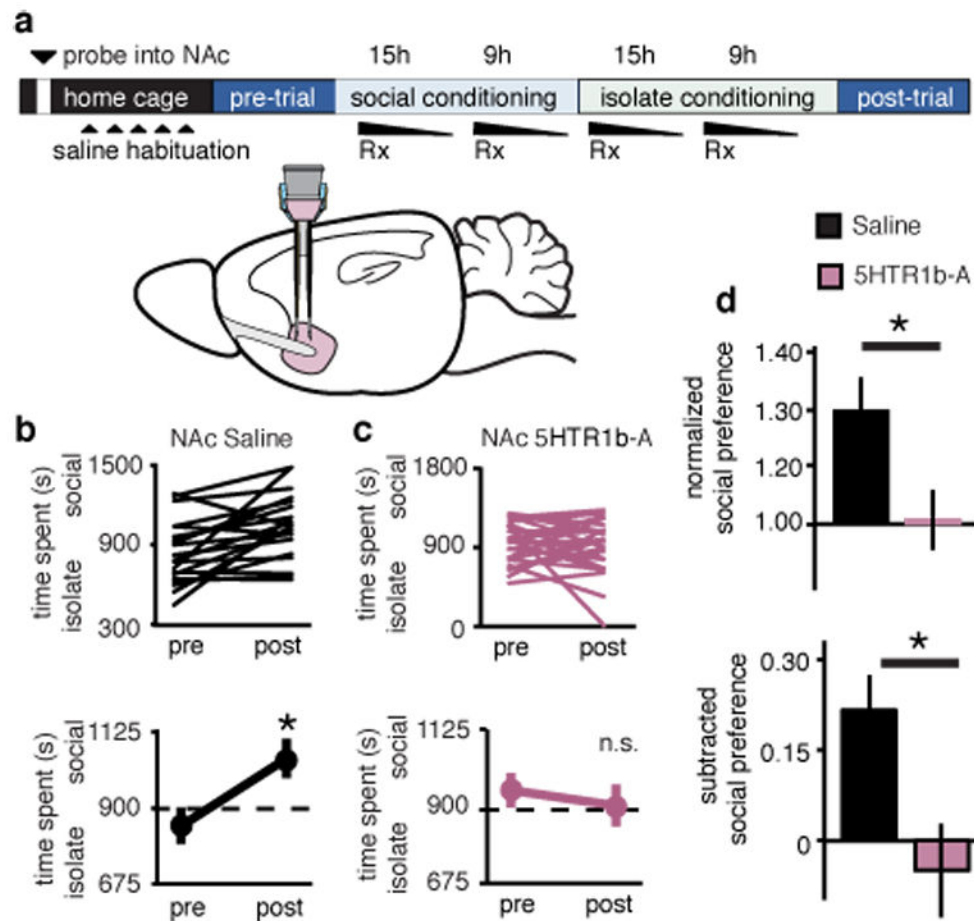


Figure 6. sCPP requires NAc 5HT1b receptors

a, Experimental time course of NAc reverse microdialysis. **b,c**, Individual (top) and average (bottom) responses in animals receiving NAc saline (**b**) versus 5HT1b-A (**c**). Saline, but not 5HT1b-A treated, animals spend more time in social bedding cue following conditioning (NAc saline, $n = 20$, NAc 5HT1b-A, $n = 26$ animals). **d**, Comparisons between treatment groups reveal significantly decreased normalized and subtracted social preference in NAc 5HT1b-A treated animals compared to saline controls. Summary data are presented as mean \pm s.e.m. (* $p < 0.05$, Student's t -test).